(12) INTERNATIONAL APPLICATION PUBLISHED UNDER THE PATENT COOPERATION TREATY (PCT)

(19) World Intellectual Property Organization
International Bureau

(43) International Publication Date
27 July 2006 (27.07.2006)

PCT

(10) International Publication Number
WO 2006/078551 A2

(51) International Patent Classification:
G01V 3/18 (2006.01)

(21) International Application Number:
PCT/US2006/001238

(22) International Filing Date: 13 January 2006 (13.01.2006)

(25) Filing Language: English

(26) Publication Language: English

(30) Priority Data:
60/644,882 18 January 2005 (18.01.2005) US
Not furnished 29 December 2005 (29.12.2005) US

(71) Applicant *(for all designated States except US)*: **BAKER HUGHES INCORPORATED** [US/US]; 3900 Essex Lane, Suite 1200, Houston, Texas 77027 (US).

(72) Inventors; and

(75) Inventors/Applicants *(for US only)*: **WANG, Tsili** [US/US]; 20723 Fawnbrook Court, Katy, Texas 77450 (US). **GEORGI, Daniel** [US/US]; 14202 Chadbourne, Houston, Texas 77079 (US).

(74) Agents: **RIDDLE, J.** et al.; BAKER HUGHER INCORPORATED, 3900 Essex Lane Suite 1200, Houston, Massachusetts 77027 (US).

(81) Designated States *(unless otherwise indicated, for every kind of national protection available)*: AE, AG, AL, AM, AT, AU, AZ, BA, BB, BG, BR, BW, BY, BZ, CA, CH, CN, CO, CR, CU, CZ, DE, DK, DM, DZ, EC, EE, EG, ES, FI, GB, GD, GE, GH, GM, HR, HU, ID, IL, IN, IS, JP, KE, KG, KM, KN, KP, KR, KZ, LC, LK, LR, LS, LT, LU, LV, LY, MA, MD, MG, MK, MN, MW, MX, MZ, NA, NG, NI, NO, NZ, OM, PG, PH, PL, PT, RO, RU, SC, SD, SE, SG, SK, SL, SM, SY, TJ, TM, TN, TR, TT, TZ, UA, UG, US, UZ, VC, VN, YU, ZA, ZM, ZW.

(84) Designated States *(unless otherwise indicated, for every kind of regional protection available)*: ARIPO (BW, GH, GM, KE, LS, MW, MZ, NA, SD, SL, SZ, TZ, UG, ZM, ZW), Eurasian (AM, AZ, BY, KG, KZ, MD, RU, TJ, TM), European (AT, BE, BG, CH, CY, CZ, DE, DK, EE, ES, FI, FR, GB, GR, HU, IE, IS, IT, LT, LU, LV, MC, NL, PL, PT, RO, SE, SI, SK, TR), OAPI (BF, BJ, CF, CG, CI, CM, GA, GN, GQ, GW, ML, MR, NE, SN, TD, TG).

Declarations under Rule 4.17:

— *as to applicant's entitlement to apply for and be granted a patent (Rule 4.17(ii))*

[Continued on next page]

(54) Title: MULTICOMPONENT INDUCTION MEASUREMENTS IN CROSS-BEDDED AND WEAK ANISOTROPY APPROXIMATION

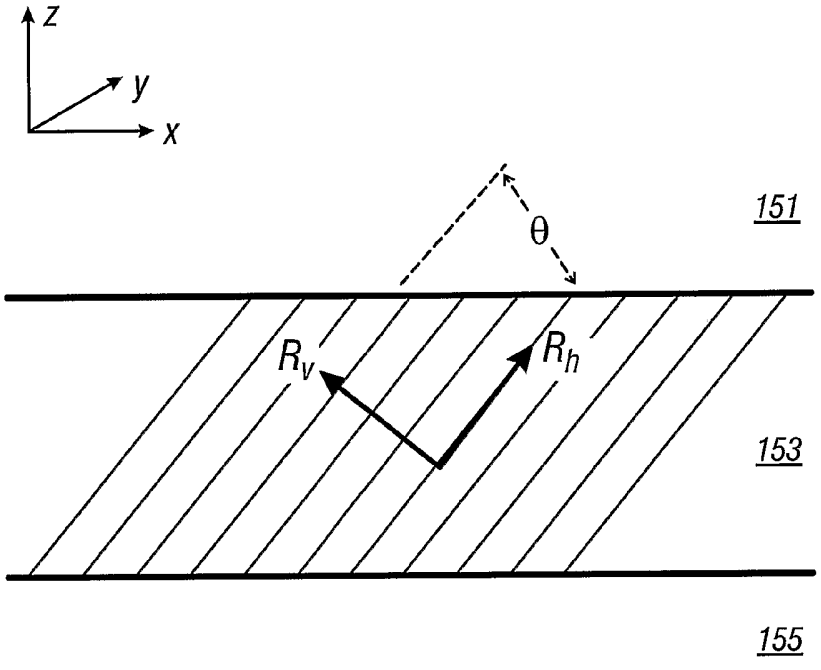

(57) Abstract: Multicomponent measurements made in a cross-bedded earth formation are processed to give one or more equivalent TI models. Resistivity information about the cross- bedding is obtained from one of the TI models and a measured cross-bedding angle. Resistivity information about the cross-bedding may also be obtained using a combination of two or more of the equivalent TI models.

WO 2006/078551 A2

— *as to the applicant's entitlement to claim the priority of the earlier application (Rule 4.17(iii))*

Published:

— *without international search report and to be republished upon receipt of that report*

For two-letter codes and other abbreviations, refer to the "Guidance Notes on Codes and Abbreviations" appearing at the beginning of each regular issue of the PCT Gazette.

MULTICOMPONENT INDUCTION MEASUREMENTS IN CROSS-BEDDED AND WEAK ANISOTROPY APPROXIMATION

Tsili Wang & Daniel T. Georgi

BACKGROUND OF THE INVENTION

1. Field of the Invention

[0001] The invention is related generally to the use of resistivity measurements for evaluation of earth formations having cross-bedding.

2. Background of the Art

[0002] Electromagnetic induction and wave propagation logging tools are commonly used for determination of electrical properties of formations surrounding a borehole. These logging tools give measurements of apparent resistivity (or conductivity) of the formation that when properly interpreted are diagnostic of the petrophysical properties of the formation and the fluids therein.

[0003] The physical principles of electromagnetic induction well logging are described, for example, in, H. G. Doll, Introduction to Induction Logging and Application to Logging of Wells Drilled with Oil Based Mud, Journal of Petroleum Technology, vol. 1, p.148, Society of Petroleum Engineers, Richardson Tex. (1949). Many improvements and modifications to electromagnetic induction resistivity instruments have been devised since publication of the Doll reference, supra. Examples of such modifications and improvements can be found, for example, in U.S. Pat. No. 4,837,517; U.S. Pat. No. 5,157,605 issued to *Chandler* et al, and U.S. Pat. No. 5,452,761 issued to *Beard* et al.

[0004] A limitation to the electromagnetic induction resistivity well logging instruments known in the art is that they typically include transmitter coils and receiver coils wound so that the magnetic moments of these coils are substantially parallel only to the axis of the instrument. Eddy currents are induced in the earth

formations from the magnetic field generated by the transmitter coil, and in the induction instruments known in the art these eddy currents tend to flow in ground loops which are substantially perpendicular to the axis of the instrument. Voltages are then induced in the receiver coils related to the magnitude of the eddy currents. Certain earth formations, however, consist of thin layers of electrically conductive materials interleaved with thin layers of substantially non-conductive material. The response of the typical electromagnetic induction resistivity well logging instrument will be largely dependent on the conductivity of the conductive layers when the layers are substantially parallel to the flow path of the eddy currents. The substantially non-conductive layers will contribute only a small amount to the overall response of the instrument and therefore their presence will typically be masked by the presence of the conductive layers. The non-conductive layers, however, are the ones which are typically hydrocarbon-bearing and are of the most interest to the instrument user. Some earth formations which might be of commercial interest therefore may be overlooked by interpreting a well log made using the electromagnetic induction resistivity well logging instruments known in the art.

[0005] U.S. Pat. No. 5,999,883 issued to *Gupta* et al, (the "Gupta patent"), the contents of which are fully incorporated here by reference, discloses a method for determination of the horizontal and vertical conductivity of anisotropic earth formations. Electromagnetic induction signals induced by induction transmitters oriented along three mutually orthogonal axes are measured. One of the mutually orthogonal axes is substantially parallel to a logging instrument axis. The electromagnetic induction signals are measured using first receivers each having a magnetic moment parallel to one of the orthogonal axes and using second receivers each having a magnetic moment perpendicular to a one of the orthogonal axes which is also perpendicular to the instrument axis. A relative angle of rotation of the perpendicular one of the orthogonal axes is calculated from the receiver signals measured perpendicular to the instrument axis. An intermediate measurement tensor is calculated by rotating magnitudes of the receiver signals through a negative of the

angle of rotation. A relative angle of inclination of one of the orthogonal axes which is parallel to the axis of the instrument is calculated, from the rotated magnitudes, with respect to a direction of the vertical conductivity. The rotated magnitudes are rotated through a negative of the angle of inclination. Horizontal conductivity is calculated from the magnitudes of the receiver signals after the second step of rotation. An anisotropy parameter is calculated from the receiver signal magnitudes after the second step of rotation. Vertical conductivity is calculated from the horizontal conductivity and the anisotropy parameter.

[0007] U.S. Patent 6,466,872 to *Kriegshauser et al.* having the same assignee as the present application and the contents of which are fully incorporated herein by reference discloses use of a multi-component logging tool for determination of anisotropic resistivity parameters of a laminated reservoir. As would be known to those versed in the art, such a laminated reservoir that has layers of different resistivities exhibits transverse isotropy even if the layers themselves are isotropic. Such a multicomponent logging tool has azimuthal sensitivity. *Kriegshauser* discloses a method of analyzing data from a multicomponent logging tool to determine water saturations of the sand and shale fractions of the reservoir. The model used in *Kriegshauser* assumes that the anisotropy axis is normal to the bedding plane. Similar models have been assumed in, for example, in US 6,618,676 to *Kriegshauser* et al., and in US 6643589 to *Zhang* et al.

[0008] Certain types of hydrocarbon reservoirs include cross-bedding wherein within geologic markers (or beds) there is additional fine bedding (cross-bedding) with a different dip than the main bedding. Cross bedding typically occur in three major environments: (1) aeolian, (2) subaqueous delta, and (3) river channels. Due to variations in grain size, cementation, water saturation and other factors, cross-bedding usually displays resistivity anisotropy (Kennedy and Herrick, 2003). On a fine scale, the resistivity perpendicular to the cross- bedding planes is in general higher than that parallel to the cross-bedding plane. Accurate reservoir evaluation and description

must consider the resistivity dependence with direction.

[0009] However, little has been understood about multicomponent induction responses in cross-bedded formations. *Anderson* et al. (1998) studied cross-bedding effects on coaxial-coil arrays but gave no results for multicomponent arrays. Difficulties arise in simulating induction response to a cross-bedded formation because, in the presence of a borehole, the problem must be dealt with as a general 3-D problem. The solution of the EM field quantities in *Anderson* takes the form of a triple Fourier integral. *Anderson* shows modeling results but provides little insight on the inverse problem of interpreting measured results even for coaxial arrays. It is desirable to reduce the complexity of the problem for numerical simulation and data interpretation. The present invention addresses this problem.

SUMMARY OF THE INVENTION

[0010] One embodiment of the invention is an apparatus for and a method of evaluating an earth formation wherein the earth formation includes cross-bedding. Multicomponent resistivity measurements are obtained in a borehole in the earth formation. The cross0beeed formation is represented by an approximate model having transverse isotropy. A parameter of the approximate model is estimated using the multicomponent measurements. The approximate model may include a bi-axially anisotropic model. The borehole may have an axis substantially normal to a main bedding of the earth formation. The method may further include determination of an angle of cross-bedding, and using the angle of cross-bedding for determining horizontal and vertical conductivities characterizing the cross-bedding. The method may further include determination of a water saturation of the cross-bedded interval, a shale fraction of the cross-bedded interval, a coarse-grained fraction of the cross-bedded interval, a fine-grained fraction of the cross-bedded interval, a permeability of a fine grained fraction of the cross-bedded interval and/or a permeability of a coarse-grained fraction of the cross bedded interval. The multi-component measurements

may include a principal component.

[0011] Another embodiment of the invention is an apparatus for evaluating an earth formation having a cross-bedded interval. A multi-component logging tool obtains multi-component measurements in a borehole in the earth formation. A processor uses an approximate model having transverse isotropy to represent the cross-bedded formation and estimates from the multicomponent measurements a parameter of the approximate model. The approximate model used by the processor may be a bi-axially anisotropic model. The borehole may have an axis substantially normal to a main bedding of the earth formation. The processor may further determine an angle of cross-bedding and use the angle of cross-bedding to estimate a horizontal conductivity and a vertical conductivity characterizing the cross-bedding. The apparatus may further include an acoustic imaging tool and/or a resistivity imaging tool and the processor may determine the cross-bedding based at least in part on an output of the imaging tool. The processor may further determine a water saturation of the cross-bedded interval, a shale fraction of the cross-bedded interval, a coarse grained fraction of the cross-bedded interval, a fine grained fraction of the cross-bedded interval, a permeability of a fine grained fraction of the cross-bedded interval, and/or a permeability of a coarse grained fraction of the cross-bedded interval. The multicomponent measurements may include a principal component. The apparatus may include a wireline, a drilling tubular or a slickline for conveying the logging tool into the borehole. The processor may be downhole, at a surface location or at a remote location.

[0012] Another embodiment of the invention is a computer readable medium for use with an apparatus for evaluating an earth formation having a cross-bedded interval. The apparatus includes a multicomponent logging tool which obtains multicomponent measurements in a borehole in the earth formation. The medium includes instructions which enable a processor to use an approximate model having transverse isotropy to represent the cross-bedded formation, and to estimate from the multicomponent

measurements a parameter of the approximate model. The medium may be a ROM, an EPROM, an EEPROM, a flash memory, and/or an optical disk.

BRIEF DESCRIPTION OF THE FIGURES

[0013] The present invention is best understood with reference to the following figures in which like numbers refer to like components and in which:

FIG. 1 (prior art) illustrates an induction instrument disposed in a wellbore penetrating earth formations;

FIG. 2 (prior art) illustrates the arrangement of transmitter and receiver coils in multicomponent induction logging tool marketed under the name 3DExplorer™;

FIG. 3 illustrates a cross-bedded model used in the method of the present invention;

FIG. 4 shows an example of horizontal and vertical resistivities resulting from thin layering of isotropic layers;

FIGS. 5a, 5b and **5c** shows H_{zz}, H_{xx} and H_{yy} responses for an exemplary cross-bedded model at different angles of cross-bedding and a frequency of 125 kHz;

FIGS. 6a, 6b show a comparison between actual H_{zz} responses and an H_{zz} response of an approximate TI model at 21kHz and 125kHz;

FIGS. 6c, 6d show a comparison between actual H_{xx} responses and an H_{yy} response of an approximate TI model at 21kHz and 125kHz;

FIGS. 6e, 6f show a comparison between actual H_{yy} responses and an H_{yy} response of an approximate TI model at 21kHz and 125kHz; and

FIG. 7 illustrates a transmitter and receiver configuration suitable for use for MWD applications.

DETAILED DESCRIPTION OF THE INVENTION

[0014] Referring now to **Fig. 1**, an electromagnetic induction well logging instrument **10** is shown disposed in a wellbore **2** drilled through earth formations. The earth

formations are shown generally at **4**. The instrument **10** can be lowered into and withdrawn from the wellbore **2** by use of an armored electrical cable **6** or similar conveyance known in the art. The instrument **10** can be assembled from three subsections: an auxiliary electronics unit **14** disposed at one end of the instrument **10**; a coil mandrel unit **8** attached to the auxiliary electronics unit **14**; and a receiver/signal processing/telemetry electronics unit **12** attached to the other end of the coil mandrel unit **8**, this unit **12** typically being attached to the cable **6**.

[0015] The coil mandrel unit **8** includes induction transmitter and receiver coils, as will be further explained, for inducing electromagnetic fields in the earth formations **4** and for receiving voltage signals induced by eddy currents flowing in the earth formations **4** as a result of the electromagnetic fields induced therein.

[0016] The auxiliary electronics unit **14** can include a signal generator and power amplifiers (not shown) to cause alternating currents of selected frequencies to flow through transmitter coils in the coil mandrel unit **8**. A processor for controlling the operation of the tool and processing acquired data may be part of the electronics unit. Alternatively, some or all of the processing and control may be done by a surface processor.

[0017] The receiver/signal processing/telemetry electronics unit **12** can include receiver circuits (not shown) for detecting voltages induced in receiver coils in the coil mandrel unit **8**, and circuits for processing these received voltages (not shown) into signals representative of the conductivities of various layers, shown as **4A** through **4F** of the earth formations **4**. As a matter of convenience the receiver/signal processing/telemetry electronics unit **12** can include signal telemetry to transmit the conductivity- related signals to the earth's surface along the cable 6 for further processing, or alternatively can store the conductivity related signals in an appropriate recording device (not shown) for processing after the instrument **10** is withdrawn from the wellbore **2**.

[0018] Referring to **Fig. 2**, the configuration of transmitter and receiver coils in the 3DExplorer™ multicomponent induction logging instrument of Baker Hughes is shown. Three orthogonal transmitters **101, 103** and **105** that are referred to as the T_x, T_z, and T_y transmitters are shown (the *z*- axis is the longitudinal axis of the tool). Corresponding to the transmitters **101, 103** and **105** are associated receivers **107, 109** and **111**, referred to as the R_x, R_z, and R_y receivers, for measuring the corresponding magnetic fields. In one mode of operation of the tool, the H_{xx}, H_{yy}, H_{zz}, H_{xy}, and H_{xz} components are measured, though other components may also be used. It should further be noted that measurements made with other coil inclinations may also be used for the method of the present invention using the well-known principles of coordinate rotation.

[0019] A cross-bedded formation is illustrated in **Fig. 3.** The upper layer **151** and the lower layer **155** are assumed to be isotropic, while the cross-bedded layer **153** is characterized by horizontal and vertical resistivities R_h and R_v parallel to and perpendicular to the cross-bedding. The cross-bedding has a normal that is inclined at an angle θ to the normal to the main bedding layers. The tool coordinate system is as shown in **Fig. 3.** θ is the angle between the cross-bedding and the main bedding (defined by the layers **151, 153, 155).**

[0020] In the cross-bedding coordinate system, the resistivity is described by the model:

$$\sigma = \begin{bmatrix} \sigma_h & 0 & 0 \\ 0 & \sigma_h & 0 \\ 0 & 0 & \sigma_v \end{bmatrix} \qquad (1),$$

where $\sigma_h = 1/R_h$, and $\sigma_v = 1/R_v$.

[0021] In the tool coordinate system (with the tool in a vertical borehole normal to the main bedding), the conductivity tensor is given by

$$\sigma^* = R\sigma R^T \quad (2),$$

where R is the rotation matrix given by

$$R = \begin{bmatrix} \cos\theta & 0 & -\sin\theta \\ 0 & 1 & 0 \\ \sin\theta & 0 & \cos\theta \end{bmatrix} \quad (3).$$

Expanding **eqn. (2)** gives

$$\sigma^* = \begin{bmatrix} \sigma_h \cos^2\theta + \sigma_v \sin^2\theta & 0 & (\sigma_h - \sigma_v)\sin\theta\cos\theta \\ 0 & \sigma_h & 0 \\ (\sigma_h - \sigma_v)\sin\theta\cos\theta & 0 & \sigma_h \cos^2\theta + \sigma_v \sin^2\theta \end{bmatrix} \quad (4).$$

Based on this, it is possible to evaluate the response of a multicomponent induction logging tool to a cross-bedded formation for various angles of cross-bedding.

[0022] The simple model in **Fig. 3** is used to demonstrate two important effects: (1) the cross-bedding effect and (2) the shoulder-bed effect. In one model, the upper and lower beds are isotropic with 1 Ω-m resistivity. To define the resistivities for the cross bedding, it is assumed that the cross bedding results from variations in grain size and associated water saturation (*Klein* et al., 1995; *Schöen* et al., 2000). It is further assumed that the sands are bimodal: the porosity is φ_1 for the coarse-grained component and φ_s for the fine-grained. The resistivities of the coarse and fine sands are given by Archie's equations:

$$R_{coarse} = R_w \frac{a}{\varphi_1^m S_{w1}^n} \quad (5), \text{ and}$$

$$R_{fine} = R_w \frac{a}{\varphi_2^m S_{w2}^n} \quad (6),$$

where R_w is the pore fluid resistivity, a is a constant, m is the porosity exponent, n is the saturation exponent, S_{w1} and S_{w2} are the water saturations. It should be noted that the use of the Archie equations is for exemplary purposes only, and that the

resistivities for the coarse- and fine-grained components could be obtained by other methods.

[0023] The R_h and R_v of the cross bedding are then given by

$$\frac{1}{R_h} = \frac{V_{coarse}}{R_{coarse}} + \frac{1 - V_{coarse}}{R_{fine}} \quad (7),$$

and

$$R_v = V_{coarse} R_{coarse} + (1 - V_{coarse}) R_{fine} \quad (8).$$

Eqns. (5)-(8) have been given by *Klein*.

[0024] **Fig. 4** shows plots of the horizontal **201** and vertical **203** resistivities, and the anisotropy ratio **205** as a function of the volume fraction of the coarse-grain sand. These are for exemplary values of R_w = 0.2Ω-m, φ_1=0.3, φ_2=0.125, S_w=S_{w1}=S_{w2}=0.6, a = 1. The resistivity values are in the coordinate system of cross-bedding. Note that R_h and R_v vary from 6.2 Ω-m to 36 Ω-m, depending on the volume fraction of coarse grains. The anisotropy ratio attains a maximum value of 2 when V_{coarse} is 0.5. In that case, R_h and R_v are approximately 10 and 20 Ω-m, respectively.

[0025] **Fig. 5a** shows the Hzz responses for three **221, 223, 225** different cross-bedding angles (0°, 30°, 60°). Here, x, y, and z are in the tool coordinate system for a vertical tool as in **Fig. 3**. The cross-bedded layer is 16 ft thick. The tool configuration is that shown in **Fig. 2** and the frequency is 125 kHz. It is noted that the Hzz response decreases in magnitude with the increasing bed dip angle, both inside and outside the cross bedded layers. This is understood because H_{zz} is largely sensitive to the horizontal resistivity in the x-direction. As the dip angle increases, the horizontal resistivity increases and H_{zz} decreases. Remarkably, the H_{zz} response varies smoothly across the boundary between the upper and lower isotropic layer and the cross-bedded layer.

[0026] The Hxx responses **231, 233, 235** shown in **Fig. 5b,** and the H_{yy} responses

241, 243, 245 shown in **Fig. 5c** increase in magnitude with the dip angle. This is understandable in view of the fact that in a vertical well H_{xx} and H_{yy} are largely inversely proportional to the vertical resistivity in the z-direction. As the dip angle increases, the vertical resistivity decreases while H_{xx} and H_{yy} increase. It is noted that the magnitudes increase both inside and outside the cross-bedded layer such that the curves for different dip angles preserve their orders. Both H_{xx} and H_{yy} exhibit transition across the bed boundaries, regardless of the cross-bedding dip angle. These sharp transitions correspond to the transmitter and/or receiver coils moving from one layer to another. The same is true at lower frequencies (not shown).

[0027] It should be emphasized that the relative dip angle in a cross-bedded formation is in general within 20-35°. The reason for simulating a much higher dip angle is that the borehole may penetrate a cross-bedded layer at an angle, making the apparent dips higher.

[0028] The above results were obtained with a 3-D modeling algorithm. Such modeling is often expensive and too time-consuming for practical data interpretation. In one embodiment of the invention, a weak-anisotropy approximation is used which simplifies the modeling and reduces the computation time. We note from field data that the small anisotropy ratio restriction is met by many multicomponent induction data seen to date.

[0029] We seek to approximate the H_{xx}, H_{yy}, and H_{zz} responses to cross bedding with those of horizontal TI media. Each TI medium has at most two distinct resistivities, one parallel and the other normal to the bed boundaries. Here, the bed boundaries are not to be confused with the cross-bedding planes. Because H_{xx}, H_{yy}, and H_{zz} have different responses to a cross-bedded formation, the approximate TI models must be different for different field components.

[0030] Our approximation consists of two steps. The first step is to ignore the off-

diagonal terms in **eqn. (4)**

$$\sigma^* = \begin{bmatrix} \sigma_x^* & 0 & 0 \\ 0 & \sigma_y^* & 0 \\ 0 & 0 & \sigma_z^* \end{bmatrix} \quad (9),$$

where

$$\sigma_x^* = \sigma_h \cos^2\theta + \sigma_v \sin^2\theta,$$
$$\sigma_y^* = \sigma_h, \quad (9a).$$
$$\sigma_z^* = \sigma_h \sin^2\theta + \sigma_v \cos^2\theta$$

Because σ_x^*, σ_y^* and σ_z^* are in general different, the new medium is biaxially anisotropic. The validity of this approximation depends on the anisotropy ratio but not on R_h or R_v individually. The approximation is valid for small anisotropy ratios (<5).

[0031] From the biaxially symmetric anisotropic medium, it is possible to build a horizontal TI model. The induction current induced by a transmitter coil tends to flow in planes parallel to the transmitter coil plane. Hence the magnitude of the induction current will be dictated primarily by the conductive components in the plane. For instance, for an x-directed transmitter, the induction current should depend mainly on σ_y^* and σ_z^*. This hypothesis roots in the long-recognized observation that the axial induction measurement in a vertical well is related only to the horizontal resistivity of the formation.

[0032] Following the above discussion, the equivalent TI models for Hxx and Hyy may be written as:

$$\sigma_{Hxx} = \begin{bmatrix} \sigma_y^* & 0 & 0 \\ 0 & \sigma_y^* & 0 \\ 0 & 0 & \sigma_z^* \end{bmatrix} \quad (10), \text{ and}$$

$$\sigma_{Hyy} = \begin{bmatrix} \sigma_x^* & 0 & 0 \\ 0 & \sigma_x^* & 0 \\ 0 & 0 & \sigma_z^* \end{bmatrix} \qquad (11).$$

[0033] For Hzz, the approximation is slightly different because the two conductivity components in the horizontal plane (σ_x^* and σ_y^*) must be reduced to one component. Using Worthington's (1981) conjecture, we calculate an effective horizontal conductivity $\sqrt{\sigma_x^*\sigma_y^*}$, and write the equivalent TI model for H_{zz} as

$$\sigma_{Hzz} = \begin{bmatrix} \sqrt{\sigma_x^*\sigma_y^*} & 0 & 0 \\ 0 & \sqrt{\sigma_x^*\sigma_y^*} & 0 \\ 0 & 0 & \sigma_z^* \end{bmatrix} \qquad (12).$$

Because Hzz does not depend on the vertical conductivity, we can simply replace the conductivity tensor with a scalar

$$\sigma_{Hzz} = \sqrt{\sigma_x^*\sigma_y^*} = \sqrt{\sigma_h\sigma_v \sin^2\theta + \sigma_h^2 \cos^2\theta} \qquad (13).$$

Eqn. (13) is the apparent conductivity formula given by *Moran and Gianzero* (1979) for coaxial-coil measurements in a deviated well. **[0031] Fig. 6a** gives a comparison of the H_{zz} component **301a, 301b** for the cross-bedded model using the approximation of **eqn (13)** with the actual response at 21 kHz. The two curves are virtually indistinguishable. **Fig. 6b** gives a comparison of the H_{zz} component **311a, 311b** for a frequency of 125kHz. Again, the two curves are virtually indistinguishable. **Figs. 6c** and **6d** give comparisons of the approximate H_{xx} component using the TI approximation and the actual results for 21 kHz and 125 kHz. **Figs. 6e** and **6f** give comparisons of the approximate H_{yy} component using the TI approximation and the actual results for 21 kHz and 125kHz.

[0034] In one embodiment of the invention, 3DEX measurements made in a near vertical borehole (normal to the bedding plane) are used to get σ_{Hzz}. An estimate of θ is obtained from measurements made with a micro-resistivity imager or an acoustic imaging tool. The estimated value of θ and the measured σ_{Hzz} may then be used to determine σ_h and σ_v, the horizontal and vertical resistivities associated with the cross bedding from **eqn. (13)**. Similar methods may be used with σ_{Hxx} and σ_{Hyy} and **eqns. (10) –(11),** or a combination of two or more of **eqns. (10)- (13)** may be used. It should be noted that if two or more of **eqns(11)- (13)** are used, then an independent measurements of the cross-bedding angle θ need not be made using an imaging tool as the system of equations enables determination of θ. Thus, it is possible to determine the cross-bedding angle and the horizontal and vertical conductivities of cross-bedding from either:

(1) determination of a TI model associated with a single principal component and an independently determined cross-bedding angle from an imaging tool, or

(2) determination of a TI model associated with two or more principal components.

[0035] Once the cross-bedding resistivity parameters have been determined, further processing may be done to determine petrophysical parameters characterizing the cross-bedding using known methods. Determination of water saturation and of fractional volumes of sand and shale components is discussed, for example, in US Patents 6711502, 6493632 and 6470274 to *Mollison* et al, having the same assignee as the present invention.

[0036] *Mollison* '274 teaches determination of the total porosity of a formation, a fractional volume of the shale, water saturation, and a resistivity of the shale in a laminated reservoir including sands that may have dispersed shales therein. A tensor petrophysical model determines the laminar shale volume and laminar sand conductivity from vertical and horizontal conductivities derived from multi-component induction log data. NMR data are used to obtain measurements of the total clay-bound water in the formation and the clay bound water in shales in the

formation. *Mollison* '502 teaches determination of the total porosity of a formation, a fractional volume of the shale, and a resistivity of the shale in a laminated reservoir including sands that may have dispersed shales therein. A tensor petrophysical model determines the laminar shale volume and laminar sand conductivity from vertical and horizontal conductivities derived from multi-component induction log data. The volume of dispersed shale and the total and effective porosities of the laminar sand fraction are determined using a Thomas-Stieber-Juhasz approach. Removal of laminar shale conductivity and porosity effects reduces the laminated shaly sand problem to a single dispersed shaly sand model to which the Waxman-Smits equation can be applied.

[0037] In one embodiment of the invention, use is made of the method taught in US6686736 to *Schoen* et al., having the same assignee as the present invention and the contents of which are incorporated herein by reference. Taught therein is a method for determining the coarse- and fine-grained fraction of a laminated sequence and estimation of permeabilities of the coarse- and fine-grained components.

[0038] One embodiment of the invention uses measurements made during drilling. United States Patent Application Ser. No. ***** filed on 9 December 2005 of *Yu* et al. under the Attorney Docket No. 414-40476 teaches the use of a tool in which a pair of z- coils is symmetrically disposed about a pair of x- coils. This is illustrated in **Fig. 7.** The tool comprises two coils **251, 251′** whose dipole moments are parallel to the tool axis direction and two coils **253, 253′** that are perpendicular to the transmitter direction. In one embodiment of the invention, the tool operates at 400 kHz frequency. When the first transmitter fires, the two receivers measure the magnetic field produced by the induced current in the formation. This is repeated for, the second transmitter. The signals are combined in following way:

$$H_{T1} = H_2 - (d_1/(d_1+d_2)^3 \cdot H_1$$
$$H_{T2} = H_1 - (d_1/(d_1+d_2))^3 \cdot H_2 \qquad (1).$$

Here, H_1 and H_2 are the measurements from the first and second receivers,

respectively, and the distances d_1 and d_2 are as indicated in **Fig. 7.** The tool rotates with the BHA and in an exemplary mode of operation, makes measurements at 16 angular orientations 22.5° apart. The measurement point is at the center of two receivers.

[0039] With the tool of **Fig. 7,** it is possible to get a full suite of measurements. Hence, 'zx' and 'xx' arrays will generate zx (xz), zy (yz), xx and yy measurements. Also, by arranging the transverse coils in orthogonal directions, we will generate xy (yx) data. Therefore, by combining zz data, we'll have a full tensor of measurement that is sufficient to resolve all resistivities and the associated dipping and inclination angles.

[0040] The invention has been described above with reference to a device that is conveyed on a wireline into the borehole. The method of the invention may also be used with a multicomponent induction logging device conveyed into a borehole on a tubular, such as a drillstring. The processing of the data may be done downhole using a downhole processor at a suitable location. It is also possible to store at least a part of the data downhole in a suitable memory device, in a compressed form if necessary. Upon subsequent retrieval of the memory device during tripping of the drillstring, the data may then be retrieved from the memory device and processed uphole.

[0041] Implicit in the control and processing of the data is the use of a computer program on a suitable machine readable medium that enables the processor to perform the control and processing. The machine readable medium may include ROMs, EPROMs, EEPROMs, Flash Memories and Optical disks.

[0042] The following definitions may be helpful in understanding the present invention:

cross-bedding: the arrangement of laminations of strata transverse or oblique to the main bedding of the strata concerned;

cross-bedding angle: angle between the cross-beds and the main beds;

EAROM: electrically alterable ROM;

EPROM: erasable programmable ROM;

flash memory: a nonvolatile memory that is rewritable;

induction: based on a relationship between a changing magnetic field and the electric field created by the change;

logging tool: The downhole hardware needed to make a log. The term is often shortened to simply "tool";

machine readable medium: something on which information may be stored in a form that can be understood by a computer or a processor;

multicomponent resistivity measurement: a measurement obtained with a different transmitter and receiver orientation; also includes measurements made with different orientations of parallel transmitter-receiver pairs;

Optical disk: a disc shaped medium in which optical methods are used for storing and retrieving information;

Principal component: measurement made with the transmitter and receiver oriented along one of the three principal directions (*x*-, *y*- and *z*-);

ROM: Read-only memory;

Resistivity: electrical resistance of a conductor of unit cross-sectional area and unit length. Determination of resistivity is equivalent to determination of its inverse (conductivity);

[0043] While the foregoing disclosure is directed to the preferred embodiments of the invention, various modifications will be apparent to those skilled in the art. It is intended that all variations within the scope and spirit of the appended claims be embraced by the foregoing disclosure.

CLAIMS

WHAT IS CLAIMED IS:

1. A method of evaluating an earth formation having a cross-bedded interval therein, the method comprising:
   (a) obtaining multicomponent measurements in a borehole in the earth formation;
   (b) representing the cross-bedded formation by an approximate model having transverse isotropy;
   (c) estimating from the multicomponent measurements a parameter of the approximate model.

2. The method of claim 1 wherein the approximate model comprises a bi-axially anisotropic model.

3. The method of claim 1 wherein the borehole has an axis substantially normal to a main bedding of the earth formation.

4. The method of claim 1 further comprising:
   (i) determining an angle of cross-bedding, and
   (ii) using the angle of cross-bedding to determine a horizontal conductivity and a vertical conductivity characterizing the cross-bedding.

5. The method of claim 4 wherein determining the angle of cross-bedding further comprises using at least one of (A) an acoustic imaging tool, and (B) a micro-resistivity imager.

6. The method of claim 4 further comprising determining at least one of (A) a water saturation of the cross-bedded interval, (B) a shale fraction of the cross-bedded interval, (C) a coarse grained fraction of the cross-bedded interval, (D) a fine grained fraction of the cross-bedded interval, (E) a permeability of a fine

grained fraction of the cross-bedded interval, and (F) a permeability of a coarse grained fraction of the cross-bedded interval.

7. The method of claim 1 wherein the multicomponent measurements comprise a principal component.

8. An apparatus for evaluating an earth formation having a cross-bedded interval therein, the apparatus comprising:
(a) a multicomponent logging tool which obtains multicomponent measurements in a borehole in the earth formation; and
(b) a processor which:
(A) uses an approximate model having transverse isotropy to represent the cross-bedded formation, and
(B) estimates from the multicomponent measurements a parameter of the approximate model.

9. The apparatus of claim 8 wherein the approximate model comprises a bi-axially anisotropic model.

10. The apparatus of claim 8 wherein the borehole has an axis substantially normal to a main bedding of the earth formation.

11. The apparatus of claim 8 wherein the processor further:
(i) determines an angle of cross-bedding, and
(ii) uses the angle of cross-bedding to estimate a horizontal conductivity and a vertical conductivity characterizing the cross-bedding.

12. The apparatus of claim 11 further comprising an imaging tool selected from the group consisting of: (I) an acoustic imaging tool, and (II) a resistivity imaging tool; and

wherein the processor determines the angle of cross-bedding based at least in part on an output of the imaging tool.

13. The apparatus of claim 11 wherein the processor further determines at least one of (I) a water saturation of the cross-bedded interval, (II) a shale fraction of the cross-bedded interval, (III) a coarse grained fraction of the cross-bedded interval, (IV) a fine grained fraction of the cross-bedded interval, (V) a permeability of a fine grained fraction of the cross-bedded interval, and (VI) a permeability of a coarse grained fraction of the cross-bedded interval.

14. The apparatus of claim 8 wherein the multicomponent measurements comprise a principal component.

15. The apparatus of claim 8 further comprising a conveyance device selected from (i) a wireline, (ii) a drilling tubular, and (iii) a slickline.

16. The apparatus of claim 8 wherein the processor is at one of (i) a downhole location, (ii) a surface location, and (iii) a remote location.

17. A computer readable medium for use with an apparatus for evaluating an earth formation having a cross-bedded interval therein, the apparatus comprising:

(a) a multicomponent logging tool which obtains multicomponent measurements in a borehole in the earth formation;

the medium comprising instructions which enable a processor to:

(b) use an approximate model having transverse isotropy to represent the cross-bedded formation, and

(c) estimate from the multicomponent measurements a parameter of the approximate model.

18. The medium of claim 17 further comprising at least one of (i) a ROM, (ii)

an EPROM, (iii) an EEPROM, (iv) a flash memory, and (v) an ptical disk.

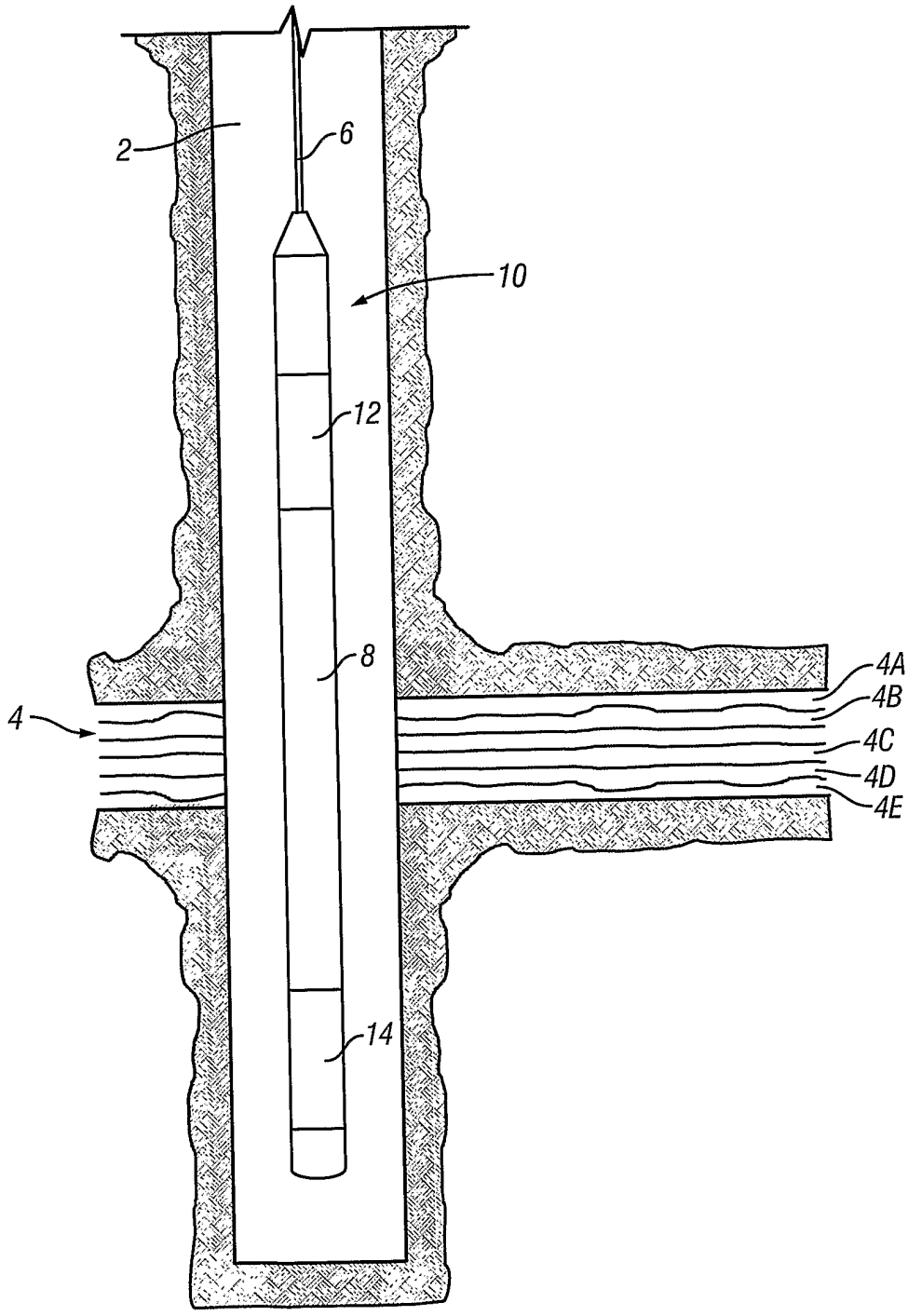

FIG. 1
(Prior Art)

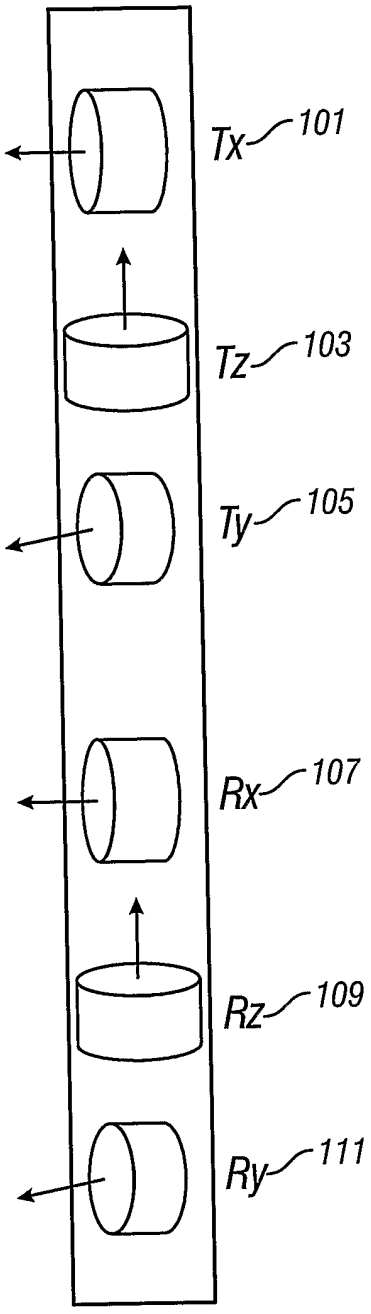

FIG. 2
(Prior Art)

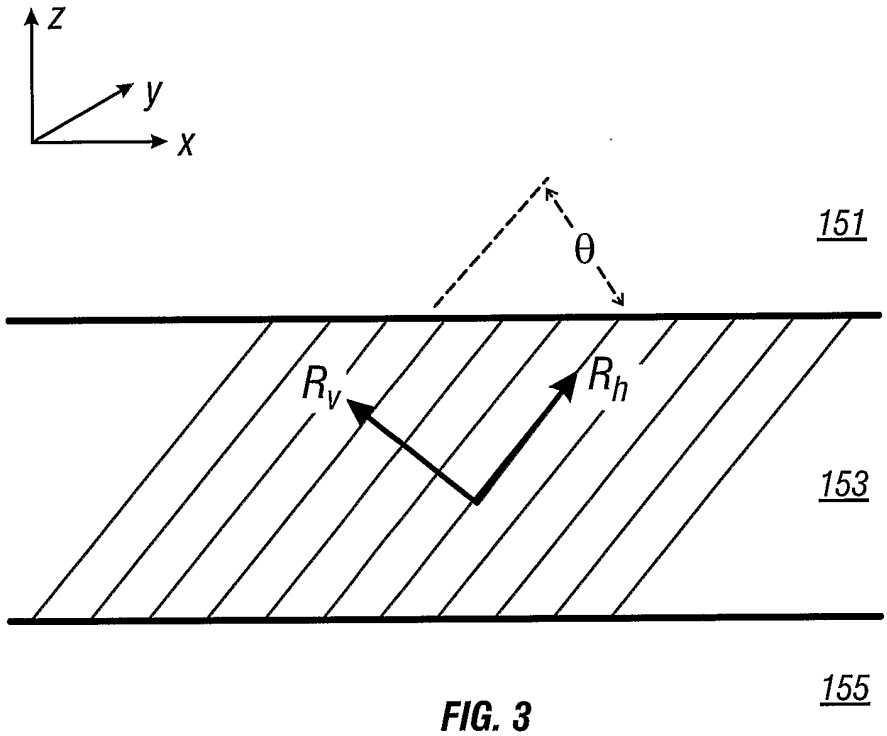

FIG. 3

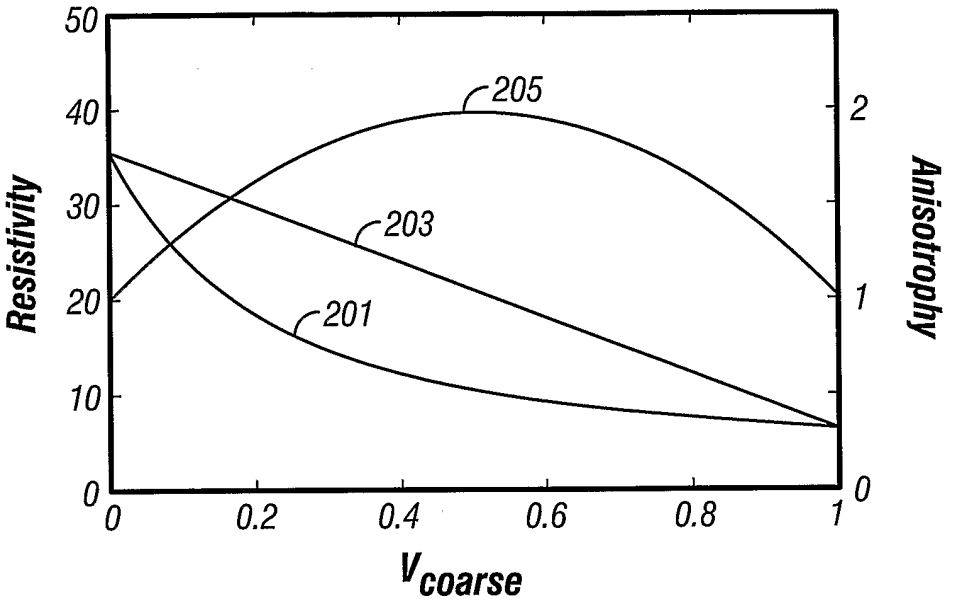
Resistivity
Anisotrophy
205
203
201
50
40
30
20
10
0
2
1
0
0
0.2
0.4
0.6
0.8
1
V_{coarse}

FIG. 4

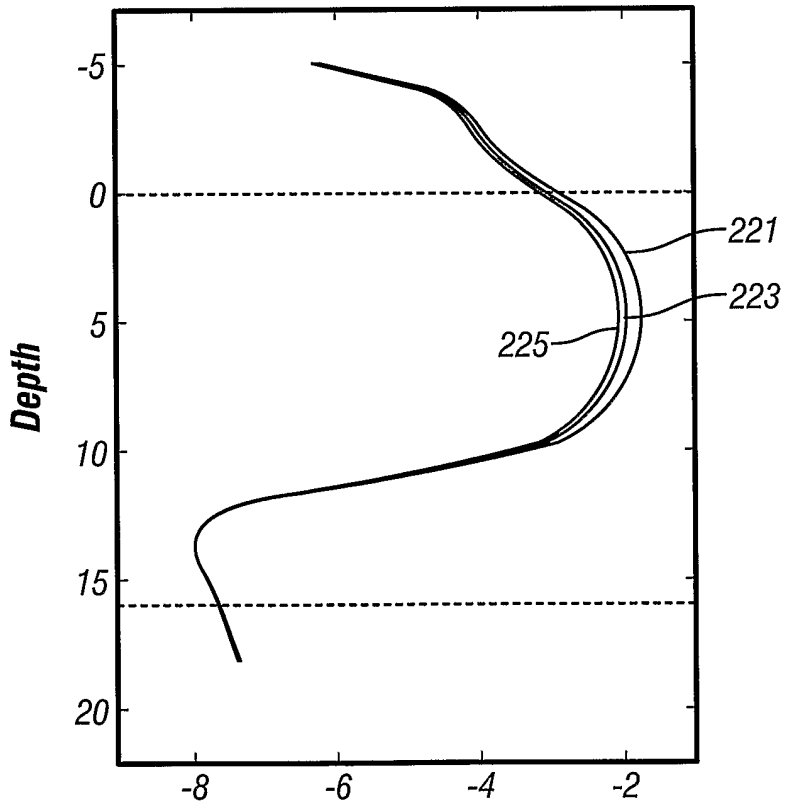
Depth
-5
0
5
10
15
20
-8
-6
-4
-2
221
223
225

FIG. 5a

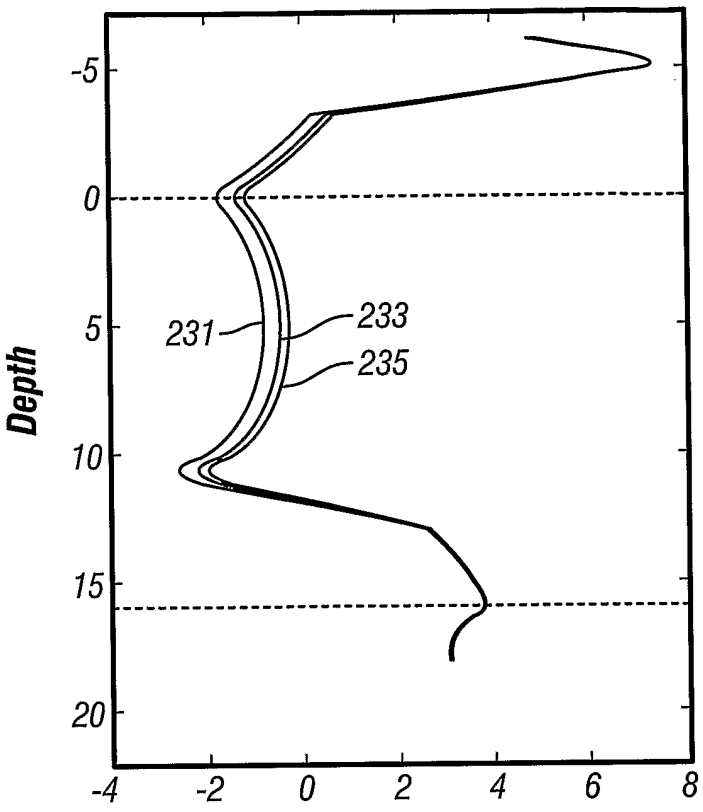
Depth
-5
0
5
10
15
20
231
233
235
-4
-2
0
2
4
6
8

FIG. 5b

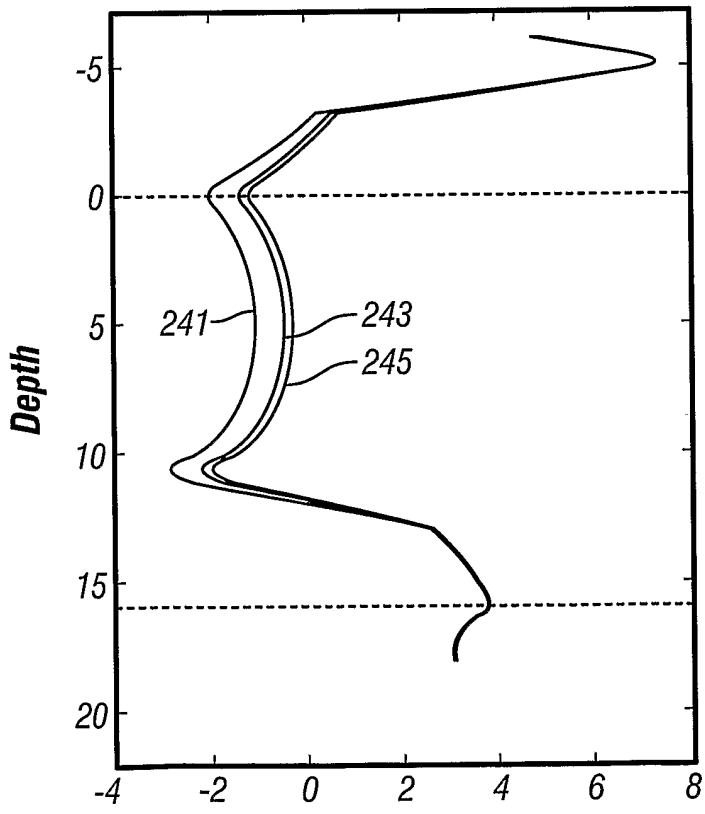
Depth
-5
0
5
10
15
20
241
243
245
-4
-2
0
2
4
6
8

FIG. 5c

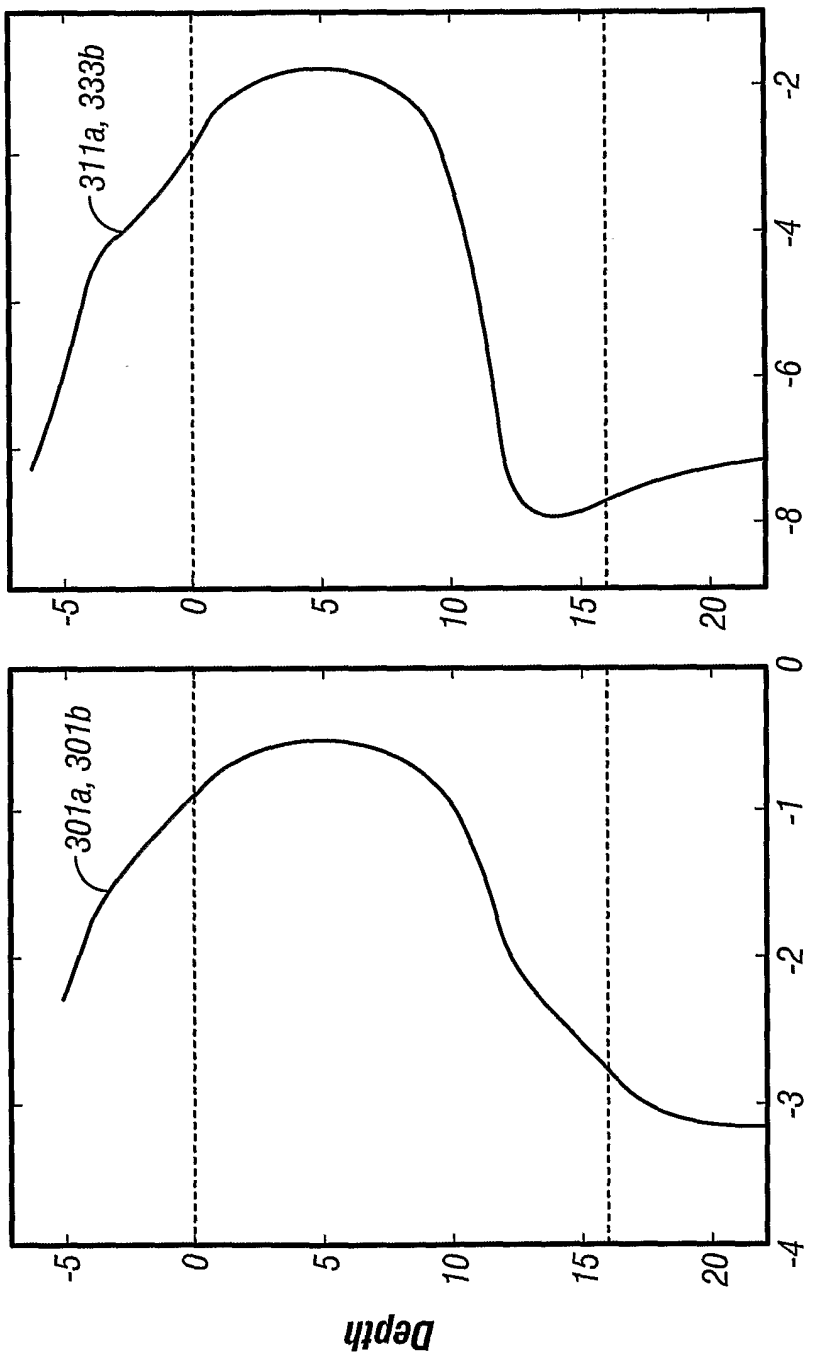

FIG. 6b

FIG. 6a

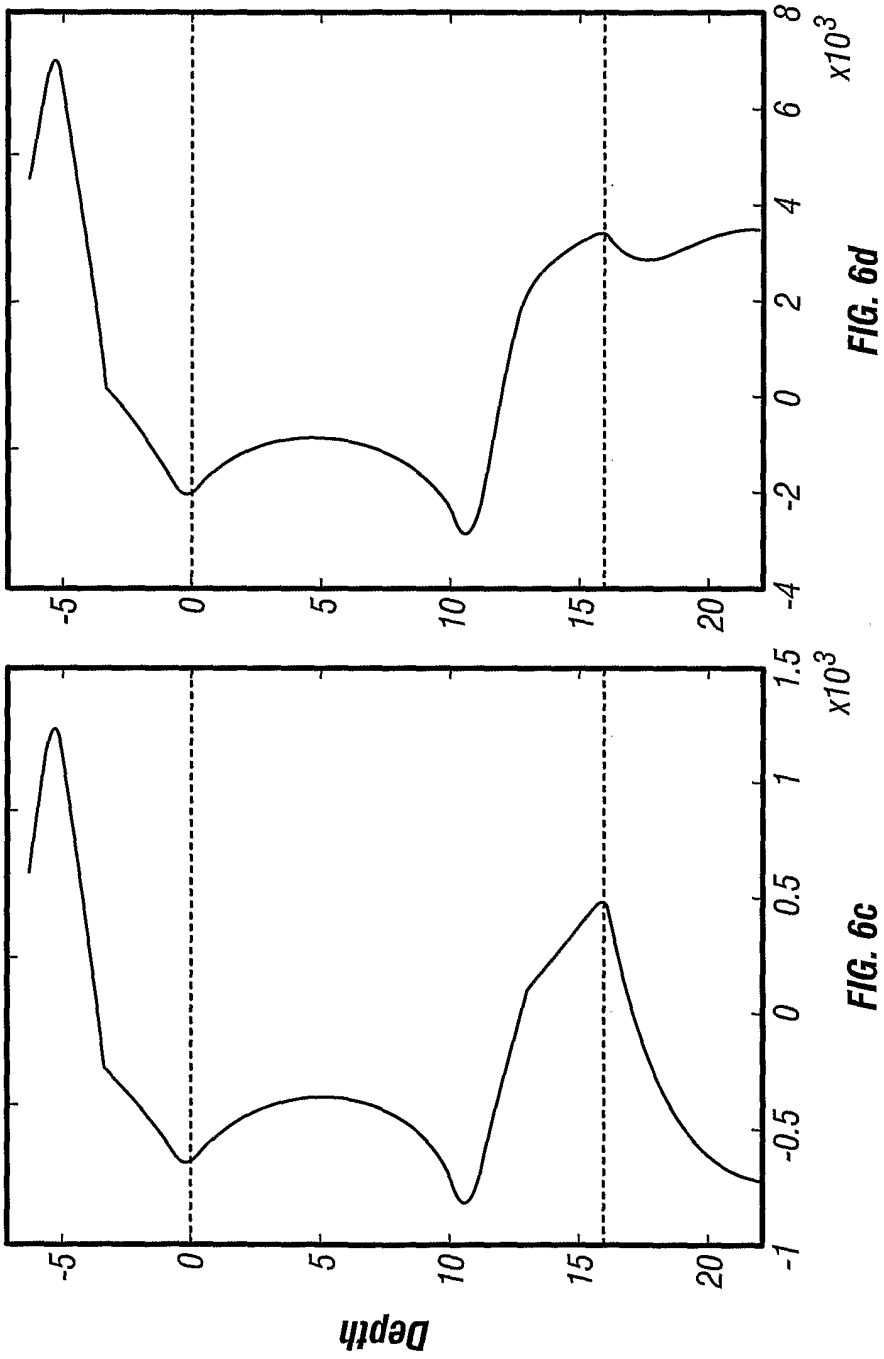

FIG. 6c

FIG. 6d

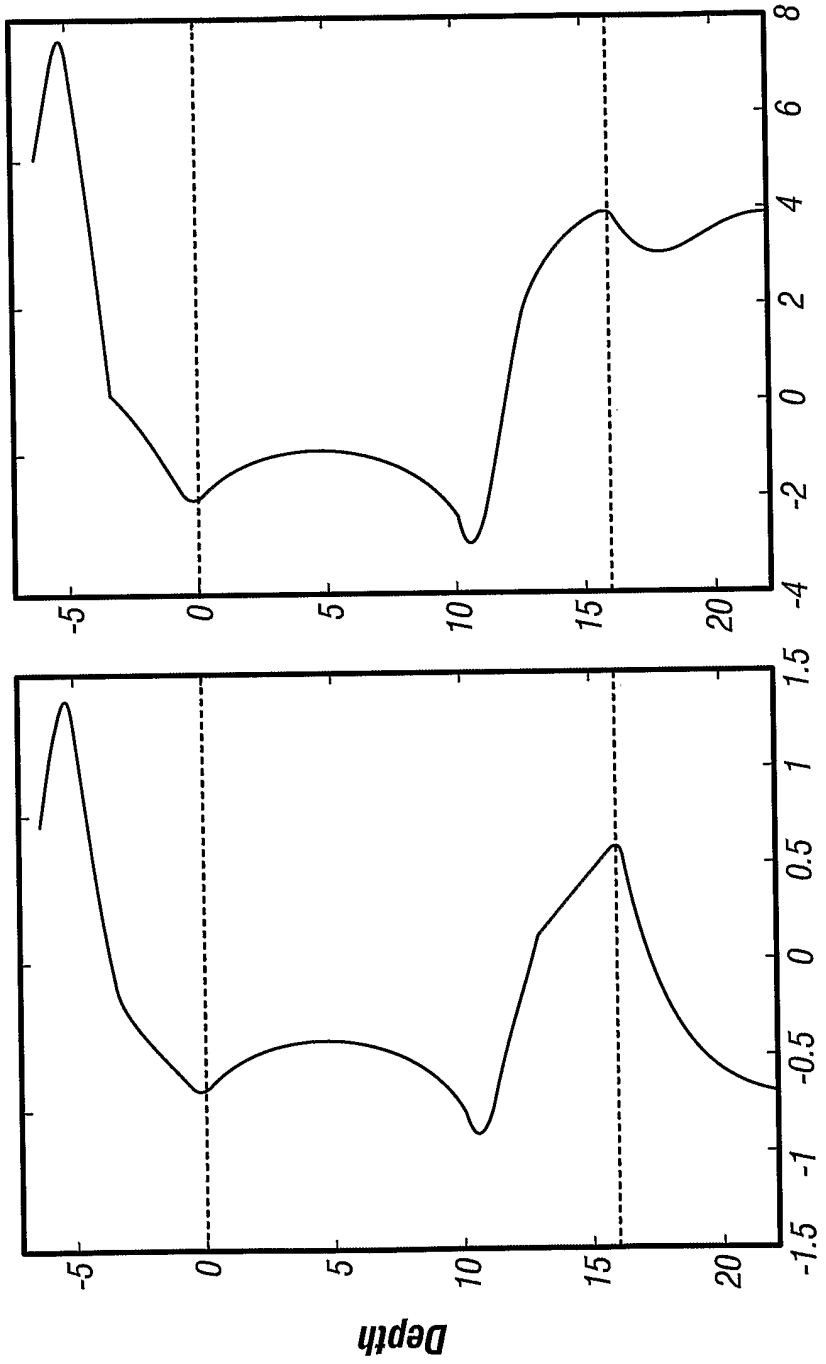

FIG. 6e

FIG. 6f

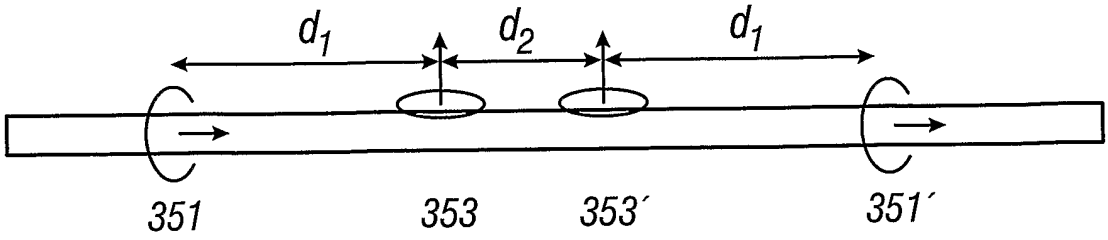

FIG. 7